



ACADEMIC  
PRESS

Available online at [www.sciencedirect.com](http://www.sciencedirect.com)

SCIENCE @ DIRECT®

Journal of Solid State Chemistry 177 (2004) 139–145

JOURNAL OF  
SOLID STATE  
CHEMISTRY

<http://elsevier.com/locate/jssc>

# Synthesis and structural study of stoichiometric $\text{Bi}_2\text{Ti}_2\text{O}_7$ pyrochlore

Andrew L. Hector\* and Seth B. Wiggin

*School of Chemistry, University of Southampton, Highfield, Southampton SO17 1BJ, UK*

Received 25 February 2003; received in revised form 10 June 2003; accepted 3 July 2003

## Abstract

$\text{Bi}_2\text{Ti}_2\text{O}_7$  has been synthesized using a co-precipitation route from  $\text{H}_2\text{O}_2/\text{NH}_3(\text{aq})$  solutions of titanium with aqueous bismuth nitrate. The stoichiometric material crystallizes into a pale yellow cubic pyrochlore phase. A powder X-ray diffraction study showed this crystallization to be very temperature sensitive, the pure phase can only be obtained within a few degrees of  $470^\circ\text{C}$ . Time-of-flight powder neutron diffraction studies of  $\text{Bi}_2\text{Ti}_2\text{O}_7$  (Space group  $Fd\bar{3}m$ ,  $a = 10.37949(4)\text{Å}$  at ambient temperature,  $Z = 8$ ,  $R_p = 3.95\%$ ,  $R_{wp} = 4.75\%$ ) revealed positional disorder in the bismuth site and in the  $\text{O}'$  oxide site both at ambient temperature and at 2 K.

© 2003 Elsevier Inc. All rights reserved.

**Keywords:** Bismuth titanate; Pyrochlore; Neutron diffraction; Disorder

## 1. Introduction

Insulating pyrochlores containing polarizable  $A$ -cations provoke extensive interest as electroceramic materials for capacitor and high-frequency filter applications. For example, bismuth zinc niobate (BZN) sinters below  $950^\circ\text{C}$ , exhibits high dielectric constants, low dielectric loss and has temperature coefficients of capacitance which are tuneable with composition [1]. The need to reduce dependence on high toxicity ceramics such as lead titanate (PT) and lead zirconate titanate (PZT) is a factor in this interest.

Pyrochlore structures have a long history and have been reviewed extensively [2]. The formula  $A_2B_2O_7$  is often expressed as  $A_2O' \cdot B_2O_6$  to emphasize the interpenetrating networks of a cuprite-like  $A_2O'$  tetrahedral net with hexagonal tungsten bronze sheets of corner sharing octahedra with  $B_2O_6$  composition. In the ideal  $Fd\bar{3}m$  cubic pyrochlore structure (Fig. 1),  $A$ ,  $B$  and  $O'$  are on special positions and the tilting of the  $BO_6$  octahedra, the  $B$ -O distance and the coordination geometry around the  $A$ -cation vary with the position of O ( $48f:x, \frac{1}{8}, \frac{1}{8}$ ).

Pyrochlores which contain  $A$ -cations with active lone pairs, such as  $\text{Sn}^{2+}$  or  $\text{Bi}^{3+}$ , often exhibit disorder in the

$A_2O'$  network. The  $A$ -cation site is a center of  $\bar{3}m$  symmetry at the center of a puckered hexagonal ring of O atoms and with two short bonds of equal length to  $O'$  along the three-fold axis. There is no obvious space to accommodate a lone pair. Birchall and Sleight [3] used Mössbauer spectroscopy to show that the isomer shift of tin niobate and tantalate pyrochlores was inconsistent with a stereochemically inactive lone pair and thus  $\text{Sn}^{2+}$  could not be located in a highly symmetric  $\bar{3}m$  environment. Further, they observed the (442) reflection in the powder X-ray diffraction pattern. This reflection has zero intensity in the ideal cubic pyrochlore structure and was modelled by an anisotropic thermal vibration at the  $A$ -cation site or (better) a disordered, static displacement of  $0.38\text{Å}$  toward the puckered ring of oxygen atoms. This displacement results in two or three shortened Sn-O distances and also accommodates the lone pair. Similarly recent studies [4] of BZN using far-infrared spectroscopy have shown a larger number of polar modes than the seven expected for an ideal pyrochlore arrangement and attributed the glass-like dielectric behavior to disorder in the  $A_2O'$  network.

It has recently been proposed that the disorder of  $A$  and  $O'$  ions is due to static displacements in all pyrochlores where the  $A$ -cation has an active lone pair [5]. This disorder has variously been modelled in bismuth pyrochlores with  $M = \text{Nb}$  [1],  $\text{Ru}$  [5],  $\text{Ti}$  [6] and  $\text{Sn}$  [7–9]. It has been noted [10,11] that in metallic

\*Corresponding author. Fax: +44-23-8059-6805.

E-mail address: [a.l.hector@soton.ac.uk](mailto:a.l.hector@soton.ac.uk) (A.L. Hector).

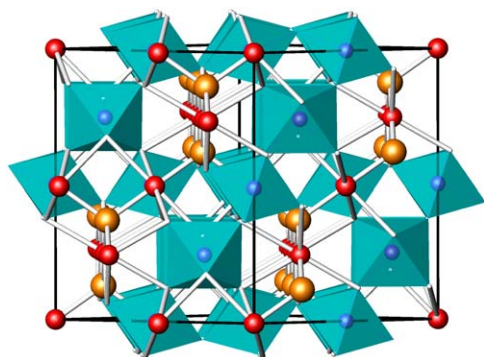


Fig. 1. Ideal cubic pyrochlore structure viewed along the (1,1,0) axis showing  $BO_6$  octahedra and the A-cation channels.

pyrochlores ( $M = \text{Rh, Ru, Ir}$ ) the lone pair character of  $\text{Bi}^{3+}$  is reduced by Bi  $6s-M$   $d$  mixing, although the bismuth site is usually still treated as disordered or with highly anisotropic thermal motion.  $\text{Bi}_2\text{Sn}_2\text{O}_7$  has a tetragonal pyrochlore structure ( $\alpha$ -phase) at ambient temperature and undergoes a phase change at around  $90^\circ\text{C}$  to  $\beta\text{-Bi}_2\text{Sn}_2\text{O}_7$  with a non-centric cubic structure [8], possibly with space group  $F\bar{4}3c$  [7].  $\gamma\text{-Bi}_2\text{Sn}_2\text{O}_7$  exists above  $690^\circ\text{C}$  with the ideal pyrochlore structure in space group  $Fd\bar{3}m$  but a disordered static displacement at the Bi site [9]. A partial structure determination of  $\text{Bi}_2\text{Hf}_2\text{O}_7$  [12] has suggested a similar distortion to that found in  $\alpha\text{-Bi}_2\text{Sn}_2\text{O}_7$ .

Pyrochlore-type bismuth titanate has a somewhat checkered history. Melt grown  $\text{Bi}_2\text{Ti}_2\text{O}_7$  single crystals with a doubled cell ( $a = 20.68 \text{ \AA}$ ) [13] were later shown [14] to be  $\text{Bi}_{1.61}\text{Zn}_{0.18}\text{Ti}_{1.94}\text{V}_{0.06}\text{O}_{6.62}$  ( $a = 10.33 \text{ \AA}$ ) plus impurities. Kahlenberg and Böhm [15] provided the first good evidence of a bismuth titanate pyrochlore as a minor phase mixed with  $\text{Bi}_2\text{Ti}_4\text{O}_{11}$  and  $\text{Bi}_4\text{Ti}_3\text{O}_{12}$  prepared at  $1100^\circ\text{C}$ . They were able to refine a lattice parameter of  $10.354 \text{ \AA}$  and to determine that the material was a bismuth deficient composition  $\text{Bi}_{1.83}\text{Ti}_2\text{O}_{6.75}$ . Slight and co-workers [6] produced nearly phase pure  $\text{Bi}_{1.74}\text{Ti}_2\text{O}_{6.62}$  at  $600^\circ\text{C}$  using precursors coprecipitated from titanium butoxide and bismuth nitrate. The lattice parameter of  $10.357 \text{ \AA}$  and the decomposition at  $650^\circ\text{C}$  to  $\text{Bi}_2\text{Ti}_4\text{O}_{11}$  and  $\text{Bi}_4\text{Ti}_3\text{O}_{12}$  fit well the previously mentioned results to indicate a material which is unstable to high temperatures and has a tendency to bismuth deficiency.

The Aurivilius phase  $\text{Bi}_4\text{Ti}_3\text{O}_{12}$  is a useful ferroelectric for high temperature ( $T_c = 675^\circ\text{C}$ ) transducers, sensors and capacitors. Mechanochemically prepared precursors to  $\text{Bi}_4\text{Ti}_3\text{O}_{12}$  crystallize via a “Bi–Ti–O fluorite” compound which decomposes to  $\text{Bi}_4\text{Ti}_3\text{O}_{12}$  at  $500\text{--}600^\circ\text{C}$  [16]. Pyrochlore and fluorite structures are very closely related (e.g.,  $\text{Sc}_2\text{Ti}_2\text{O}_7$  has an anion deficient fluorite structure [2]) and this bismuth-rich fluorite phase has a similar temperature stability to  $\text{Bi}_2\text{Ti}_2\text{O}_7$ . Polycrystalline thin films of composition  $\text{Bi}_2\text{Ti}_2\text{O}_7$  [17]

have high permittivity and low leakage current. They have been used to improve the electrical properties of  $\text{Bi}_4\text{Ti}_3\text{O}_{12}$  [17] and PZT [18] ferroelectric thin films and are considered promising gate materials for advanced MOS transistors [19]. In view of these promising applications, further detail of the temperature stability and structure of materials with this composition is timely. For example, a recent study examined the dielectric and ferroelectric properties of crystallographically uncharacterized “ $\text{Bi}_2\text{Ti}_2\text{O}_7$ ” after sintering at  $1150\text{--}1200^\circ\text{C}$  [20] at which temperature the sample probably consisted of  $\text{Bi}_4\text{Ti}_3\text{O}_{12}$  and  $\text{Bi}_2\text{Ti}_4\text{O}_{11}$  [6,15].

Aqueous solutions of titanium can be prepared by the dissolution of titanium powder in hydrogen peroxide/ammonia mixtures. This has previously been used [21] to produce PT and PZT powders at low temperature by coprecipitation with aqueous lead and zirconyl nitrates. The advantage is that organics and halides are avoided so the materials can be fired at lower temperature. Adapting this route to the bismuth titanate system we have produced materials with controlled bismuth content and we report here the synthesis and a detailed structure study of stoichiometric  $\text{Bi}_2\text{Ti}_2\text{O}_7$ .

## 2. Experimental

$\text{Bi}_2\text{Ti}_2\text{O}_7$  samples were prepared by co-precipitation of a basic titanium solution with an acidic bismuth solution. Titanium metal (0.252 g, 5.2 mmol) with a particle size of  $250 \mu\text{m}$  was added to a mixture of hydrogen peroxide (28%, 21 g, 0.18 mmol) and ammonia solution (34%, 6 g, 0.12 mmol). The stirred mixture was maintained at just below room temperature using a water bath and the titanium dissolved over a period of 3–4 h, resulting in a bright yellow solution. This was added quickly to a stirred solution of bismuth nitrate pentahydrate (2.53 g, 5.2 mmol) in  $1.2 \text{ mol dm}^{-3}$   $\text{HNO}_3$  ( $50 \text{ cm}^3$ ), initially forming a dark orange solution with vigorous evolution of gas. With continued stirring a pale cream precipitate soon formed, this was stirred for 30 min to agglomerate the particles and ensure complete precipitation. After filtering and washing with dilute ( $\sim 10\%$ ) ammonia the cream-colored solid was dried at  $50^\circ\text{C}$ . In order to minimize loss of bismuth through volatilization, samples were calcined as pressed disks between  $400^\circ\text{C}$  and  $500^\circ\text{C}$  for various time periods (see results section). These were stacked in an alumina crucible, which was placed into a closed crucible containing powdered  $\text{Bi}_2\text{O}_3$ .

All samples were characterized by powder X-ray diffraction using a Bruker D8 diffractometer with  $\text{CuK}\alpha_1$  radiation. Phases present were identified by comparison with the PDF2 database [22]. The sample used for the main structural study was analyzed by EDX using a Philips ESEM 2600 with EDAX Phoenix

detector. Area scans on several pressed pellet samples showed Bi:Ti ratios of 1:1.00(3). This sample was analyzed gravimetrically in duplicate for titanium by digesting a 0.5 g sample in hot  $\text{HNO}_3$  (4 mold  $\text{m}^{-3}$ , 100  $\text{cm}^3$ ), filtering the resulting white  $\text{TiO}_2$  and drying to constant weight at 300°C. %Ti = 16.5(2) (calculated value is 15.3%). Powder neutron diffraction data were collected in 10 mm vanadium cans using the high-resolution time-of-flight HRPD diffractometer at the ISIS facility. Data were collected for 10 h each at 2 K and ambient temperature. Data from the backscattered bank ( $2\theta = 168.33^\circ$ ) with a time-of-flight range of 33–120  $\mu\text{s}$  ( $d = 0.684\text{--}2.48 \text{ \AA}$ , 108 reflections) were refined using the GSAS package [23] using a cosine Fourier series background function with 10 parameters and exponential pseudovoigt profile coefficients (GSAS type 3).

### 3. Results and discussion

#### 3.1. Synthesis

The rationale of our approach was to apply organic-free methods used successfully to synthesize PT and PZT materials at low temperature [21] to the synthesis of  $\text{Bi}_2\text{Ti}_2\text{O}_7$ . We then planned to carry out high temperature ammonolysis reactions of these precursors to obtain oxide nitrides, however, it rapidly became clear that reduction to bismuth metal was the only reaction which would occur under these conditions. In terms of the production of  $\text{Bi}_2\text{Ti}_2\text{O}_7$ , this method appears to give complete control of the Bi:Ti stoichiometry of the as-precipitated material. The filtrate was evaporated (after treating with  $\text{MnO}_2$  to decompose the remaining  $\text{H}_2\text{O}_2$ ) and no Bi or Ti could be detected by EDX in the  $\text{NH}_4\text{NO}_3$  residue.

Samples were calcined at various temperatures to determine the stability range of the pyrochlore material. Fig. 2 shows the PXD patterns of samples calcined for 16 h at selected temperatures. The surprise finding is that the stability range is so narrow. At 470°C the  $\text{Bi}_2\text{Ti}_2\text{O}_7$  pyrochlore phase is pure by PXD. A temperature increase of just 10°C results in formation of  $\text{Bi}_4\text{Ti}_3\text{O}_{12}$  impurity and a sample calcined at 500°C contained 19%  $\text{Bi}_4\text{Ti}_3\text{O}_{12}$  according to a multi-phase refinement of the PXD data. Reducing the calcination temperature by 10°C results in a very poorly crystalline sample, at 450°C the sample is amorphous. Prolonged annealing at 460°C (96 h) did lead to crystalline  $\text{Bi}_2\text{Ti}_2\text{O}_7$  but with  $\text{Bi}_4\text{Ti}_3\text{O}_{12}$  impurity.

The material produced here is markedly different from the  $\text{Bi}_{1.74}\text{Ti}_2\text{O}_{6.62}$  of Sleight [6], which could be annealed at 600°C. Refinement of the PXD data of our 470°C-annealed product yielded a cubic lattice parameter of 10.376 Å, an increase over the 10.357 Å

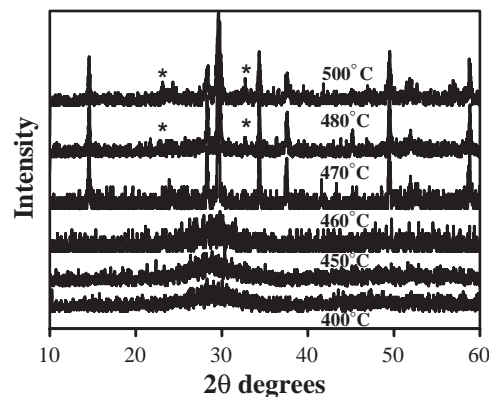


Fig. 2. Variation in powder X-ray diffraction patterns of  $\text{Bi}_2\text{Ti}_2\text{O}_7$  with annealing temperature. Most intense reflections of the  $\text{Bi}_4\text{Ti}_3\text{O}_{12}$  impurity are marked\*.

reported for  $\text{Bi}_{1.74}\text{Ti}_2\text{O}_{6.62}$ . EDX indicates a composition  $\text{Bi}_2\text{Ti}_2\text{O}_7$  but the gravimetric Ti content is slightly high. It is possible that the samples contain some Ti-rich amorphous material due to bismuth loss by volatilization, though if so this was not sufficient to be observed as a “hump” in the diffraction backgrounds. It is likely that the previous synthesis route [6] could only obtain a bismuth deficient material because of the need to heat strongly enough to remove organics. Our material is more temperature sensitive so requires a precursor system, which decomposes fully below its annealing temperature of 470°C.

#### 3.2. Initial PND structure study

The sample used for PND experiments (approximately 8 g) was produced as described in the experimental section but with the amount of each reagent increased by a factor of 5. The precursor was calcined as a single stack of pellets at 470°C for 16 h.

Initial refinements used the ideal pyrochlore structure (Bi at (0, 0, 0), Ti at ( $\frac{1}{2}$ ,  $\frac{1}{2}$ ,  $\frac{1}{2}$ ), O at ( $\frac{1}{8}$ ,  $\frac{1}{8}$ ,  $x$ ) and O' at ( $\frac{1}{8}$ ,  $\frac{1}{8}$ ,  $\frac{1}{8}$ )) in space group  $Fd\bar{3}m$  with isotropic thermal parameters on all atoms. A reasonable fit to most of the pattern was obtained with data collected at 2 K and at ambient temperature but with very high thermal parameters on Bi and O' ( $U_{\text{iso}} = 0.077, 0.039 \text{ \AA}^2$ , respectively, at 2 K). The (442) reflection (at  $d = 1.73 \text{ \AA}$ ) was observed. As previously discussed, this reflection is not allowed in the pyrochlore structure with isotropic thermal parameters, but becomes allowed on occupation of a 32- or 96-fold site. It usually indicates [1,5–7,9] anisotropy or a static displacement at the A-cation site. Anisotropic refinement of the Bi thermal parameters resulted in a marked improvement in the fit ( $\chi^2$  fell from 10.65 to 5.47) with severe broadening perpendicular to the (111) axis, toward the puckered ring of O atoms. Anisotropic thermal parameters on the

Ti and O sites yielded a further improvement ( $\chi^2 = 5.29$ ).

Next we tested a static displacement of bismuth atoms with isotropic thermal parameters using the 96*g* ( $x, x, z$ ) or 96*h* ( $0, y, -y$ ) sites. These sites correspond to a displacement toward the center of each pair of O atoms or toward each O atom (respectively) in the puckered ring. Either way the result is a ring of scattering density around the central bismuth site, it has been pointed out by Avdeev [5] that these sites overlap strongly and may be indistinguishable. The structure of  $\text{Bi}_{1.74}\text{Ti}_2\text{O}_{6.62}$  was found to be better described using the 96*h* site [6]. With our compounds the 96*g* site yielded slightly better statistics than the 96*h* ( $\chi^2 = 4.83$  vs. 4.86) and so was used subsequently, though the difference is probably insignificant. The improvement over a description of the bismuth site with anisotropic thermal parameters, however, is significant and a reasonable bismuth thermal parameter ( $U_{\text{iso}} = 0.004 \text{ \AA}^2$  at 2 K) was obtained. The remaining anomaly in the refinements was a high  $O'$  thermal parameter ( $U_{\text{iso}} = 0.059 \text{ \AA}^2$  at 2 K), this will be dealt with in the next section.

Some weak reflections were still not accounted for. These were attributed to the vanadium sample holder (2.14, 1.51 and 1.23 Å) and a small amount of  $\text{Bi}_4\text{Ti}_3\text{O}_{12}$  (peaks at 2.26 and 1.92 Å are the strongest in the PND pattern of this phase and are of <1% intensity in our diffraction patterns). Generated PND patterns showed that no impurity peaks of significant intensity coincide with reflections due to  $\text{Bi}_2\text{Ti}_2\text{O}_7$ . They were ignored, being too weak to sensibly model as a second phase.

Fig. 3 places the room temperature lattice parameter of  $\text{Bi}_2\text{Ti}_2\text{O}_7$  (10.379 Å) into the context of a number of other pyrochlore phases. The most obvious observation is that  $\text{Bi}_2\text{Zr}_2\text{O}_7$  should form under appropriate soft synthetic conditions. Similarly  $\text{Nd}_2\text{Ti}_2\text{O}_7$ , though low temperature crystallization of a lanthanide titanate is unlikely to be achieved. A “Pyrochlore stability field” based on the relative cation ionic radii has previously been used to describe which compositions form. Values of  $r_A/r_B = 1.46$ –1.78 at atmospheric pressure have been

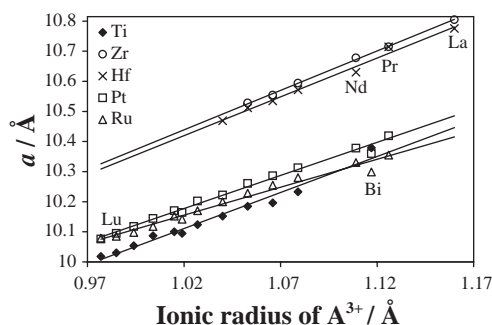


Fig. 3. Graph of ambient temperature lattice parameter [2] against  $A$ -cation ionic radius [20] for selected  $A_2^{3+}M_2^{4+}O_7$  pyrochlores ( $A$  = rare earth or bismuth).

quoted [2] with higher values obtainable at high pressure. For the rare earth titanates,  $r_A/r_B$  varies between 1.61 ( $\text{Lu}_2\text{Ti}_2\text{O}_7$ ) and 1.78 ( $\text{Sm}_2\text{Ti}_2\text{O}_7$ ) [24]. The larger rare earths (Nd–La) have not been shown to form Pyrochlore-type titanates.  $\text{Bi}_2\text{Ti}_2\text{O}_7$ , with  $r_A/r_B = 1.93$ , falls outside this stability field although  $\text{Bi}_{1.85}\text{Rh}_2\text{O}_{6.83}$  ( $r_A/r_B = 1.95$ ) is known [11].

Kennedy [11] has provided a useful discussion of the variation in the effective ionic radius of  $\text{Bi}^{3+}$  between insulating and metallic pyrochlores. In the metallic compounds ( $M = \text{Rh, Ru, Ir, Pt}$ ) the lattice parameter is systematically smaller than predicted by  $A$ -cation ionic radius, (Fig. 3 shows Pt and Ru). In the insulators,  $\text{Bi}_2\text{Ti}_2\text{O}_7$  and  $\alpha$ - $\text{Bi}_2\text{Sn}_2\text{O}_7$  the lattice parameter is larger than expected ( $\text{Bi}_2\text{Sn}_2\text{O}_7$  is the tetragonal  $\alpha$ -phase at ambient temperature so an effective cubic parameter was considered, for  $\text{Bi}_2\text{Hf}_2\text{O}_7$  the effective lattice parameter of 10.86 Å [12] is much bigger than expected and has been omitted from Fig 3). In this work we have shown that the lattice parameter of stoichiometric  $\text{Bi}_2\text{Ti}_2\text{O}_7$  is significantly larger than previously reported so the effect is more marked. Variations in the  $\text{Bi}^{3+}$  ionic radius due to  $\text{Bi } 6s$ – $M d$  mixing are well known [10] and can significantly reduce the lone pair character of the  $\text{Bi } 6s$  orbital in the metallic phases, explaining this variation. We note there is also a correlation to the displacement of bismuth from the ideal site. In  $\text{Bi}_2\text{Ti}_2\text{O}_7$ , bismuth is displaced by 0.43 Å and in BZN [1] the displacement is 0.39 Å. In the metallic phase  $\text{Bi}_2\text{Ru}_2\text{O}_7$  a static displacement of only 0.16 Å has been refined [5] whereas in the rhodate [11], iridate [25] and platinate [26] phases refinement with anisotropic Bi has been adequate. The distorted pyrochlore structures of  $\alpha/\beta$ - $\text{Bi}_2\text{Sn}_2\text{O}_7$  and  $\text{Bi}_2\text{Hf}_2\text{O}_7$  could well result from ordering due to a large Bi displacement.

### 3.3. Positional disorder on the $O'$ site

The isotropic thermal parameter on  $O'$  was found to be very high before and after disordering of the Bi site. The  $O'$  site is of  $43m$  symmetry and is inconsistent with anisotropic thermal motion, so the high thermal parameter can indicate a reduced occupancy or some disorder on this site. The analytical data showed a 1:1 ratio of Bi:Ti and refinement of the Bi or Ti occupancy resulted in values higher than 1 and negative thermal parameters. Refinement of the  $O'$  occupancy resulted in a value of  $\sim 0.9$  but  $U_{\text{iso}}$  was still high ( $\sim 0.05 \text{ \AA}^2$ ) and a deficiency at this site is chemically non-sensible without a corresponding deficiency at a cation site. Similar results were obtained with data collected at 2 K and at ambient temperature.

Disorder of  $O'$  can be achieved using a number of different sites.  $O'$  is located at the center of a tetrahedron formed by the ideal bismuth sites. The  $32e$  ( $x, x, x$ ) site represents a displacement either toward (or away from)

each vertex of the tetrahedron, this site has been used to describe the  $O'$  displacement in  $\text{Bi}_2\text{Ru}_2\text{O}_7$  [5] and in  $\gamma\text{-Bi}_2\text{Sn}_2\text{O}_7$  [7]. The  $48f$  ( $x, \frac{1}{8}, \frac{1}{8}$ ) site will displace  $O'$  toward the center of each edge of the tetrahedron.  $96g$  ( $x, x, z$ ) displaces  $O'$  to a site roughly toward (and simultaneously away from) half of the bismuth sites described by the  $96g$  bismuth displacement, this was used in BZN [1] where it was specifically related to localized Bi:Zn ordering.  $96h$  has a similar effect to  $96g$  but with a  $30^\circ$  rotation around the three-fold axis. A static displacement of  $O'$  (with an appropriate fractional occupancy) on each of these four positions was tried. In all cases a reduced thermal parameter was found initially but refinement of the position moved the atom toward the central position and the thermal parameter refined to a high value. Thus the refinements were highly unstable, even with the highest level of damping.

The position of  $O'$  was then explored using  $\delta F$  Fourier maps. The  $O'$  atom was removed from the refinement and the nuclear density around the  $O'$  position was calculated. The plots showed a definite tetrahedral shape, consistent with occupation of the  $32e$  site. However, in contrast with the published structure of  $\text{Bi}_2\text{Ru}_2\text{O}_7$  [5], a displacement away from each of the ideal Bi positions was observed. A static displacement was revisited but with the same problems as previously described. The nuclear density in the  $\delta F$  was highest at the center of the tetrahedron and a static displacement does not appear to be a good description, even at 2 K. Manually moving  $O'$  from the central position in steps the refinement statistics deteriorated progressively. However, the tetrahedral shape cannot be described by a normal ellipsoidal distribution. The best fit we have been able to obtain is with a combination of the ideal  $8a$  and the tetrahedrally disordered  $32e$  site with the overall stoichiometry constrained. This corresponds to a fairly mobile  $O'$  oxygen with some tendency to associate more closely with any three of the four bismuth sites. With this model the refinement was stable, converging

smoothly, and the isotropic thermal parameters, whilst still high, became more reasonable ( $U_{\text{iso}} \sim 0.04 \text{ \AA}^2$ ).

In  $\text{Bi}_2\text{Ti}_2\text{O}_7$  we observe a similar displacement of  $O'$  to that reported for  $\text{Bi}_2\text{Ru}_2\text{O}_7$  [5], but the displacement is away from an individual Bi rather than toward one. A plausible explanation lies in the magnitude of the Bi displacement from the ideal position. Bi lies  $0.43 \text{ \AA}$  from the three-fold axis and so a displacement of  $O'$  along this axis will not increase its association with Bi to the same extent as in  $\text{Bi}_2\text{Ru}_2\text{O}_7$  where the displacement is only  $0.16 \text{ \AA}$ . An individual oxygen can be closely associated with three Bi atoms ( $\text{Bi}-O' = 2.01 \text{ \AA}$  at 2 K) if it is displaced in the opposite direction and if all three Bi atoms are displaced toward the axis. The presence of a second harmonic signal in the  $^{119}\text{Sn}$  Mössbauer spectrum of tin niobate and tantalate pyrochlores [3], demonstrates that static  $\text{Sn}^{2+}$  displacements must be cooperative for a large enough domain to destroy the site centricity. A cooperative Bi displacement here will result in a closer association with one of the  $O'$  atoms. Pyrochlore BZN has a glass-like dielectric behavior

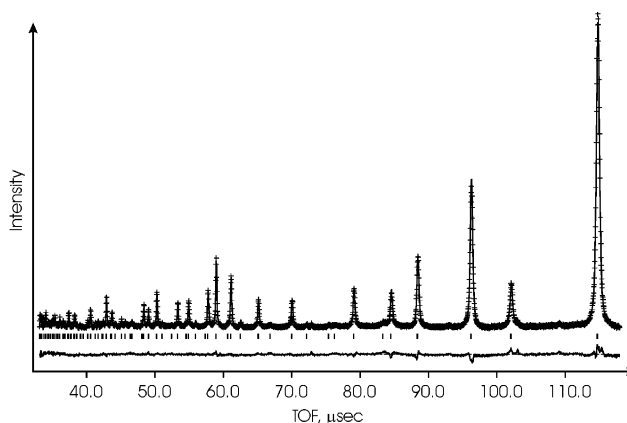


Fig. 4. Final profile fit to the 2K PND data. Crosses are observed intensities, the upper continuous line the calculated profile and the lower continuous line is the difference. Tick marks give the reflection positions in  $Fd\bar{3}m$ .

Table 1  
Refined crystallographic parameters for  $\text{Bi}_2\text{Ti}_2\text{O}_7$  in space group  $Fd\bar{3}m$

Atom	Site	$x$	$y$	$z$	$U_{11}, U_{22}$	$U_{33}$	$U_{12}$	$U_{13}, U_{23}$	FRAC
Bi	$96g$	0.0167(4)	0.0167	-0.0357(4)	0.12(6)	0.12	0	0	1/6
		0.0173(3)	0.0173	-0.0342(3)	1.13(4)	1.13	0	0	1/6
Ti	$16d$	1/2	1/2	1/2	0.10(6)	0.10	0	0	1
		1/2	1/2	1/2	1.30(5)	1.30	-0.31(5)	-0.31	1
O	$48f$	1/8	1/8	0.43128(8)	1.08(3)	0.53(5)	-0.93(6)	0	1
		1/8	1/8	0.43153(5)	1.81(2)	1.34(3)	-0.90(5)	0	1
$O'(1)$	$8a$	1/8	1/8	1/8	4.05(13)	4.05	0	0	0.896(7)
		1/8	1/8	1/8	4.43(10)	4.43	0	0	0.872(5)
$O'(2)$	$32e$	0.215(3)	0.215	0.215	4.05(13)	4.05	0	0	0.026(2)
		0.219(2)	0.219	0.219	4.43(10)	4.43	0	0	0.032(1)

Top row refers to data collected at 2 K, bottom row at ca 290 K. Estimated standard deviations are given in parentheses and thermal displacement parameters are in units of  $\text{Å}^2 \times 100$ .

2 K:  $a = 10.35907(5) \text{ \AA}$ ,  $\chi^2 = 3.82$ ,  $R_{\text{wp}} = 4.53\%$ ,  $R_{\text{p}} = 3.85\%$ .

290 K:  $a = 10.37949(4) \text{ \AA}$ ,  $\chi^2 = 2.95$ ,  $R_{\text{wp}} = 4.75\%$ ,  $R_{\text{p}} = 3.95\%$ .

which has been explained by local hopping of atoms in the  $A$  and  $O'$  positions between several potential minima [4], this effectively means that the domains are in a constant state of flux. The need for  $O'$  to occupy both the central position and the displaced position could indicate either that the ordered domains in  $\text{Bi}_2\text{Ti}_2\text{O}_7$  are relatively short-lived or that the domains are smaller than in the compounds which show a static  $O'$  displacement.

### 3.4. Structure description

The final refined structure parameters are shown in Table 1 and the final fit at 2 K is shown in Fig. 4.

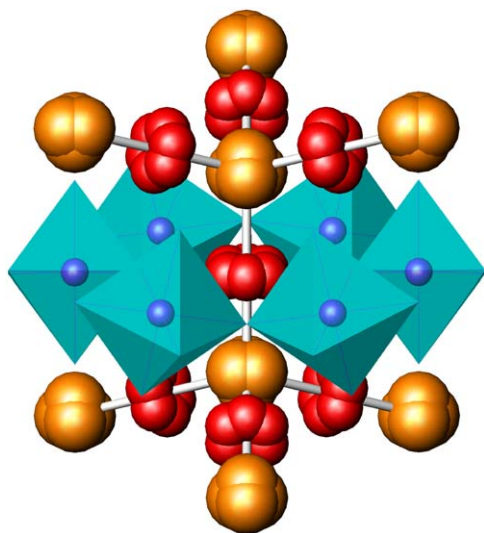


Fig. 5. Schematic structure of  $\text{Bi}_2\text{Ti}_2\text{O}_7$  showing the six-fold static disorder at Bi and the four-fold disorder at  $O'$ .

Fig. 5 shows the disorder at Bi and  $O'$  schematically, note the close association of a displaced  $O'$  to one of the disordered Bi sites in each ring. The  $\text{TiO}_6$  trigonal antiprism and  $\text{BiO}_6\text{O}'_2$  scalenohedron are shown in Fig. 6. Further details of the crystal structure investigations can be obtained from the Fachinformationszentrum Karlsruhe, 76344 Eggenstein-Leopoldschafen, Germany (fax: +49-7247-808-666; [mailto:crysdata@fiz.karlsruhe.de](mailto:mailto:crysdata@fiz.karlsruhe.de)) on quoting the depository numbers CSD-413013 or CSD-413014 for  $\text{Bi}_2\text{Ti}_2\text{O}_7$  at 290 or 2 K, respectively.

The Ti site has reasonable anisotropic thermal parameters at 290 K, the O thermal parameters are slightly high but not enough to consider a displacement as used with  $\gamma\text{-Bi}_2\text{Sn}_2\text{O}_7$  [7]. At 2 K a non-positive definite anisotropic thermal parameter was obtained for Ti and so this atom was refined with isotropic thermal parameters. The 2 K Ti–O distance of 1.964 Å is consistent with the reported values for the lanthanide titanate pyrochlores which range [27] from 1.936 Å (Dy) to 1.973 Å (Sm). At 2 K the Ti–O–Ti angle is 137.51(4)° and Bi–O–Ti is 96.15(5)°, 104.46(5)° or 113.64(6)°.

The  $O'$  thermal parameters change little on cooling from 290 to 2 K. Temperature factor coefficients should decrease linearly with temperature and the high values of these parameters may indicate some further level of disorder.

Bond-valence calculations (Calculated using VaList program [28]; bond valence data used in these calculations taken from Ref. [29]) were used to evaluate the effect of the bismuth displacement. The bond valence sum (BVS) for  $\text{Ti}^{4+}$  was found to be 4.00. Displaced bismuth with  $O'$  in the central position results in a  $\text{Bi}^{3+}$  BVS of 3.01 whereas the ideal pyrochlore structure, with no bismuth or oxygen displacements, results in a  $\text{Bi}^{3+}$

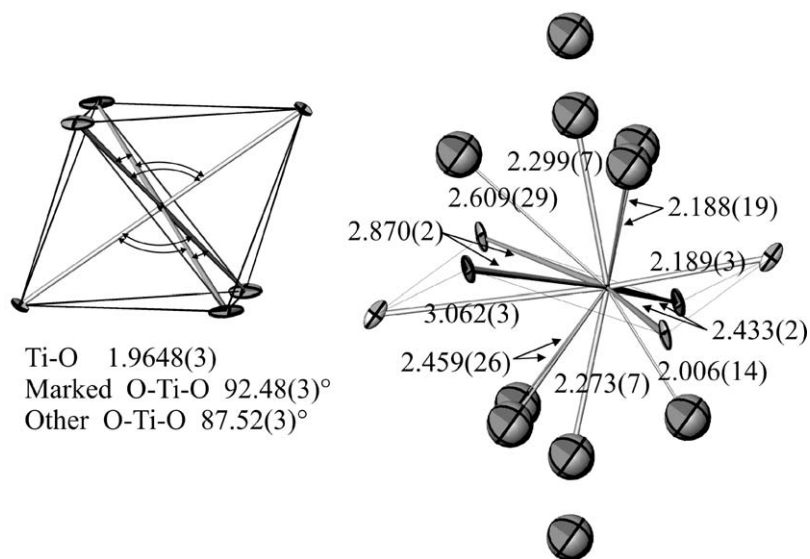


Fig. 6. Cation coordination spheres in  $\text{Bi}_2\text{Ti}_2\text{O}_7$  with selected bond lengths (Å) and angles at 2 K. In the bismuth sphere (right) only one of the six disordered Bi sites is shown but all the possible  $O'$  sites are included.

BVS of 2.73. The effect of the  $O'$  displacements is also interesting,  $\text{Bi}^{3+}$  BVS values can vary from 1.85 to 3.87 depending on the oxygen position. This also reinforces the idea that the displacements must be cooperative within domains such that one  $\text{Bi}-O'$  is shortened and the other is lengthened in order to satisfy the coordination requirements of the  $\text{Bi}^{3+}$ .

#### 4. Conclusions

Stoichiometric  $\text{Bi}_2\text{Ti}_2\text{O}_7$  has been produced and been shown to have a cubic pyrochlore structure with static bismuth displacements and probable domains of static  $O'$  displacements. The displacements are similar to those observed in BZN (but larger) which is a useful electroceramic, however to use  $\text{Bi}_2\text{Ti}_2\text{O}_7$  it would be necessary to anneal it to high density. This would be impossible from powder samples because it has a low decomposition temperature. If the films of this composition which are produced by CVD have this structure, or if suitable sol–gel processes can be developed, these could provide attractive low cost electroceramic materials with only moderate toxicity.

#### Acknowledgments

We thank the Rutherford Appleton Laboratory for the provision of ISIS beamtime, R.M. Ibberson for assistance with data collection and M.T. Weller for useful discussions. ALH is grateful to the Royal Society for support through a University Research Fellowship.

#### References

- [1] I. Levin, T.G. Amos, J.C. Nino, T.A. Vanderah, C.A. Rendall, M.T. Lanagan, *J. Solid State Chem.* 168 (2002) 69–75.
- [2] M.A. Subramanian, G. Aravamudan, G.V. Subba Rao, *Prog. Solid State Chem.* 15 (1983) 55–143.
- [3] T. Birchall, A.W. Sleight, *J. Solid State Chem.* 13 (1975) 118–130.
- [4] S. Kamba, et al., *Phys. Rev. B* 66 (2002) 054106(1–8); J.C. Nino, M.T. Lanagan, C.A. Randall, S. Kamba, *Appl. Phys. Lett.* 81 (2002) 4404–4406.
- [5] M. Avdeev, M.K. Haas, J.D. Jorgensen, R.J. Cava, *J. Solid State Chem.* 169 (2002) 24–34.
- [6] I. Radosavljevic, J.S.O. Evans, A.W. Sleight, *J. Solid State Chem.* 136 (1998) 63–66.
- [7] B.J. Kennedy, Ismunandar, M.M. Elcombe, *Mater. Sci. Forum* 278–281 (1998) 762–767.
- [8] R.D. Shannon, J.D. Bierlein, J.L. Gillson, G.A. Jones, A.W. Sleight, *J. Phys. Chem. Solids* 41 (1980) 117–122.
- [9] R.H. Jones, K.S. Knight, *J. Chem. Soc. Dalton Trans.* (1997) 2551–2555.
- [10] R.D. Shannon, *Acta Crystallogr. Sect. A* 32 (1972) 751–767.
- [11] B.J. Kennedy, *Mater. Res. Bull.* 32 (1997) 479–483.
- [12] S.L. Sorokina, A.W. Sleight, *Mater. Res. Bull.* 33 (1998) 1077–1081.
- [13] S. Shimada, K. Kodaira, T. Matshushita, *J. Cryst. Growth.* 41 (1977) 317–320.
- [14] V. Kahlenberg, H. Böhm, *J. Alloys Compd.* 223 (1995) 142–146.
- [15] V. Kahlenberg, H. Böhm, *Cryst. Res. Technol.* 30 (1995) 237–241.
- [16] J.G. Lisoni, P. Millán, E. Vila, J.L. Martín de Vidales, T. Hoffmann, A. Castro, *Chem. Mater.* 13 (2001) 2084; A. Castro, P. Millán, L. Pardo, B. Jiménez, *J. Mater. Chem.* 9 (1999) 1313–1317.
- [17] S.W. Wang, W. Lu, N. Li, Z.F. Li, H. Wang, M. Wang, X.C. Shen, *Mater. Res. Bull.* 37 (2002) 1691–1697.
- [18] S.W. Wang, H. Wang, S. Shang, J. Huang, Z. Wang, M. Wang, *J. Cryst. Growth* 217 (2000) 388–392.
- [19] S.W. Wang, H. Wang, X.M. Wu, S.X. Shang, M. Wang, Z.F. Li, W. Lu, *J. Cryst. Growth* 224 (2001) 323–326.
- [20] S.P. Yordanov, I. Ivanov, Ch.P. Carapanov, *J. Phys. D: Appl. Phys.* 31 (1998) 800–806.
- [21] E.R. Camargo, J. Frantti, M. Kakihana, *J. Mater. Chem.* 11 (2001) 1875–1879.
- [22] PCPDFWIN Version 2.2, Powder Diffraction File, International Centre for Diffraction Data, Swarthmore, PA, 2001.
- [23] R.B. Von Dreele, A.C. Larson, GSAS general structure analysis system, Neutron Scattering Centre, MS-H805, Los Alamos National Laboratory, Los Alamos, NM, 2001.
- [24] N.E. Brese, M. O'Keeffe, *Acta Crystallogr. Sect. B* 47 (1991) 192–197.
- [25] B.J. Kennedy, *J. Solid State Chem.* 123 (1996) 14–20.
- [26] E. Beck, S. Kemmler-Sack, *J. Less-Common Metals* 135 (1987) 257–268.
- [27] V.V. Nemoshkalenko, S.V. Borisenko, V.N. Uvarov, A.N. Yaresko, A.G. Vakhney, A.I. Senkevich, T.N. Bondarenko, V.D. Borisenko, *Phys. Rev. B* 63 (2001) 075106(1–8).
- [28] A.S. Wills, I.D. Brown, VaList, CEA, France, 1999, Program available from author at [willsas@netscape.net](mailto:willsas@netscape.net)
- [29] I.D. Brown, D. Altermatt, *Acta Crystallogr. B* 41 (1985) 244–247.